JOURNAL OF SOLID STATE CHEMISTRY 56, 379–389 (1985)

Structural Study of Gels of V_2O_5: Vibrational Spectra of Xerogels

L. ABELLO, E. HUSSON, Y. REPELIN, AND G. LUCAZEAU

Laboratoire de Chimie-Physique du Solide, Université Paris XIII, 93430 Villetaneuse, France

Received May 21, 1984; in revised form September 17, 1984

A complete vibrational study of xerogels of vanadium oxide corresponding to the formula $V_2O_5 \cdot nH_2O$ with $n = 1.6, 1.2, 0.6, 0.4$, and 0.3, was performed. Raman and infrared spectra of powder and oriented films of the samples have been recorded at 100 and 300 K. It has been possible to verify the existence of two different structures. For $n \simeq 0.3$, V_2O_5 layers are connected as in the crystal through V=O—V bonds, each water molecule trapped into cavities being linked by its two hydrogen atoms to the oxygen lattice, the interlayer distance (*b* parameter) should be close to that of the crystal. For $n = 0.6$, the V_2O_5 layers are not connected as in the crystal through the long V—O bonds, but the vanadium atoms are coordinated to H_2O molecule by V—OH_2 bonds. For $0.6 < n < 1.4$ three kinds of water molecules are likely present. Finally, it is shown that the conclusions are consistent with the literature structural models proposed from diffraction methods.

I. Introduction

The electronic properties of gels of vanadium oxide have stimulated a large number of recent studies on this system. The gels can be obtained by two methods: (i) the amorphous V_2O_5 is dissolved in water (noted gels A) and (ii) by the polymerization of the decavanadic acid (noted gels P).

The gels obtained by the second method have given rise to recent structural studies (*1–5*) and for this reason we shall limit this study to gels P. The comparison between gels P and gels A is discussed by Abelb and Lucazeau (*15*).

Abello and Pommier, from precise DTA and TG (slow heating rate) measurements (*6*) have shown that the water contents characterized by $n = 0.3$, $n = 0.6$, and $n = 1.4$ correspond to specific compounds. The $n = 0.3$ content appears as a limit below which the crystallization occurs. In this respect it must be underlined that these two compositions (0.3 and 0.6) differ from those ($n = 0.1$ and $n = 0.5$) reported by Aldebert *et al.* (*1*), the rapid heating rate used in their study could explain this discrepancy. Abello *et al.* have shown that for the composition $n = 1.4$ three different types of water molecules can be considered. Figure 1 sums up this discussion. The swelling of gels by water with $0 < n < 20$ has been studied by X-ray diffraction and by wide angle neutron scattering by Aldebert *et al.* (*5*); it has been shown that the first stages of hydration is stepwise. Electronic and X-ray diffraction measurements had led Legendre *et al.* (*2, 3*) to propose a description of the long- and short-range order for the $n = 1.6$ and $n = 0.5$ compounds but the water molecules were not definitively placed. However, the $n = 0.3$ limit compound was not investigated and the aim of the present work is to study the structure of this gel and

0022-4596/85 $3.00

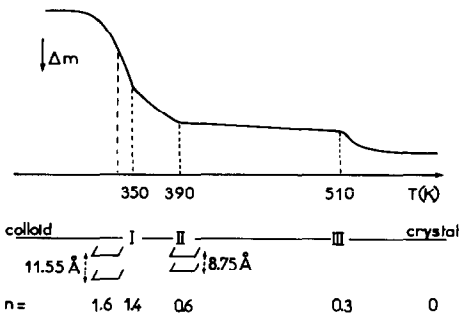

FIG. 1. TG curve corresponding to the dehydration of a $V_2O_5 \cdot nH_2O$ gel (*6*) from $n = 4$ to $n = 0$.

to check for $n = 1.6$ and $n = 0.6$ to what extent the short-range order model proposed form diffraction methods is compatible with the vibrational results, with a particular emphasis on the Raman results, the sensitivity of this technique to short-range structure being well known. This work is the continuation of a previous ir–Raman study on a V_2O_5 single crystal (*7*) and on amorphous and water-rich gels of V_2O_5 (*8*).

The experimental results are presented and discussed in the present paper. The normal mode calculations which have been performed on the structural models discussed here will be reported in a forthcoming paper (*9*). The prominent results of this study have been presented recently (*10, 11*); since an infrared study of water in V_2O_5, $n = 1.6$ and 0.5 H_2O, has been published (*12*).

II. Experimental

1. Samples

The vanadium pentoxide gels are prepared by polymerization of decavanadic acid. A yellow solution of decavanadic acid is obtained from metavanadate solution in contact with an acid-exchange resin (*13*). This solution polymerizes spontaneously at room temperature in a few hours and one can obtain gels with a composition of about 300 parts H_2O per 1 part V_2O_5. Above 1100 H_2O one obtains a colloidal solution. The xerogels are obtained by evaporation of water, they correspond to a water content comprised between 1.6 and 0.3 H_2O per V_2O_5. At room temperature this evaporation leads to a gel with the approximate formula $V_2O_5 \cdot 1.6\ H_2O$. A further dehydration can be achieved under vacuum ($\simeq$0.6 H_2O) or by heating the sample up to 0.3 H_2O, the hydration–dehydration is reversible for $n \geq 0.6$; for $n \leq 0.3$ the hydration does not occur any more. The precise water content of our samples were obtained by TG measurements (*6*).

2. Infrared Spectra

A Perkin–Elmer 580 spectrometer was used. The samples were studied as Nujol or Fluorolube mulls or dispersed in CsI. Films of xerogels were obtained by evaporation of gels on AgBr. This substance is inert toward V_2O_5 even when it is heavily hydrated (which is not the case for KBr or even CsI) and allows to investigate the range 4000–200 cm^{-1}.

3. Raman Spectra

Samples have been recorded on a triple-monochromator Raman spectrometer using the 647.1-nm exciting line of a krypton laser. The samples have been studied either as powders or as films evaporated on the external surface of glass tubes maintained in rotation in order to prevent the laser heating of the sample.

For powder samples, the different compositions have been obtained by heating a tube, containing a gel, for several hours at the appropriate temperatures (473, 423, 373, 340, and 300 K), corresponding to $n =$ 0.3, 0.4, 0.6, 1.2, and 1.6 compositions, respectively. The tubes were sealed *in situ* and then cooled down. For the films the sample was maintained at the appropriate temperature during the recording of the spectra.

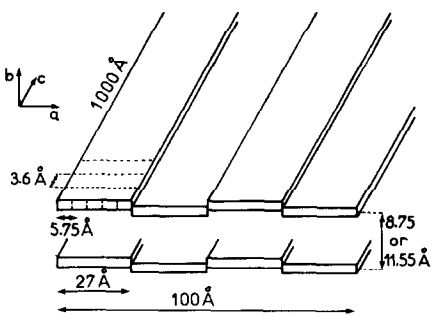

FIG. 2. Schematic representation of the ribbon structure of V_2O_5 xerogels [after Legendre *et al.* (*2, 3*)].

III. Structural Considerations and Selection Rules

1. Literature Models

$V_2O_5 \cdot 1.6\ H_2O$: Legendre and Livage (*2*) have shown from electron microscope experiments that this compound is made up of entangled fibers. These fibers can be described as ribbons of 1.000×100 Å. A two-dimensional periodical structure with $a = 27$ Å and $c = 3.6$ Å closely related to the crystalline V_2O_5 has been proposed and each ribbon should be made of fibrils of a width equal to 27 Å connected to each other by sharing water molecules. The organization of the ribbon in a direction perpendicular to the plane of the ribbon has been deduced from X-ray diffraction (*1, 3*). Each interribbon distance being of 11.55 Å. This model is sketched in Fig. 2.

$V_2O_5 \cdot 0.5\ H_2O$: the structure of the V_2O_5 framework is the same as above, however the interribbon distance decreases to 8.75 Å.

$V_2O_5 \cdot 0.3\ H_2O$: as already mentioned there are no structural informations on this phase.

2. Selection Rules

The discussion of the spectra refers to three basic structures: (i) the orthorhombic D_{2h}, V_2O_5 crystal, (ii) one independent 2D layer of a D_{2h} symmetry, and (iii) the quasi-one-dimensional fibril presented above.

The number and the activity of the $k = 0$ normal modes of the two first structures are identical and have been already reported in (*7*), however the suppression of interlayer bondings can introduce some frequency shifts in the case of the independent layer. We shall limit this section to the classification of the modes of the isolated fibril.

If we consider that the fibril is of infinite length (the c parameter is taken equal to 3.6 Å as in the V_2O_5 crystal), the vibrational modes are those of a one-dimensional crystal. There are now five V_2O_5 per unit cell and thus 2.5 times more ($k = 0$) modes are expected than for the crystal or for the independent layer containing two formulas per unit cell.

All the vibrational modes become ir and Raman active and under the C_s group they can be classified as

$$\Gamma_{opt} = \Gamma_x - \Gamma_{Tx,y,z} = 70\,A' + 35\,A'' - (2\,A' + A'')$$

when one takes into account the three zero frequency translations. The rotations of the fibril as a whole are expected at very low frequencies.

In the crystal (D_{2h}) we have shown in Table 1 of Ref. (*7*) that each internal mode of a V_2O_5 unit gives rise to doublets because of the coupling between the two V_2O_5 units of the unit cell. In the present model one expects that two internal modes give rise to five "crystal modes." Moreover, it is well known, as far as the local geometry is kept, that, in a first approximation, a local activity (ir or Raman) can be ascribed to one given internal mode and that it determines the activity of the normal modes of the structure. As an example if we consider the stretching ν(V=O) internal mode, the strongly Raman active crystal mode of Ag symmetry at 994 cm^{-1} is expected to generate Raman active modes in the fibril, recip-

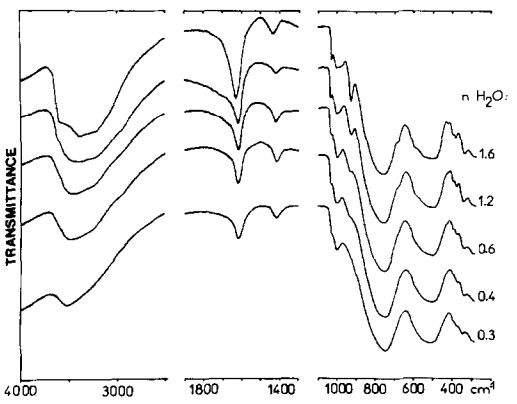

FIG. 3. Infrared spectra of different films of xerogels deposited on an AgBr disk, containing 1.6, 1.2, 0.6, 0.4, and 0.3 H_2O per V_2O_5, respectively. In order to attenuate the dichroic effects, the angle between the normal **N** to the sample surface and the ir beam direction θ = (**N**, **I**), was taken equal to $\theta \simeq 15°$.

rocally the internal modes which do not involve a large polarizability change in the crystal are expected to remain quasi-inactive in the fibril whatever the symmetry might be. Most of the new frequencies are expected to fall into a narrow frequency range centered around those of the crystal. However, new defects modes can be expected such as those associated with free terminal atoms resulting from the breaking of V–O bonds when going from the 3D crystal to 1D fibril. Finally, "local modes" resulting from the specific interactions between H_2O and V_2O_5 frame can also be expected.

IV. Experimental Results and Discussion

Infrared and Raman spectra of gels n = 1.6, 1.2, 0.6, 0.4, and 0.3 are presented in Figs. 3, 4, and 5, respectively. The polarized Raman spectra of an oriented film of the 1.6 H_2O gel are reported in Fig. 6. The ir OH stretching region of $VOSO_4 \cdot 3\ H_2O$ and $VOSO_4 \cdot 1.5\ H_2O$ (*14*) are given for comparison in Fig. 7. The ir dichroic effects are illustrated in Fig. 8.

1. Raman

(*a*) *Evidence of two limit compositions: n = 0.3 and n = 0.6.* The evolution of Raman spectra from n = 0 (crystal) to n = 1.6 (see Fig. 5) is described in terms of crystal bands which persist through all compositions, and

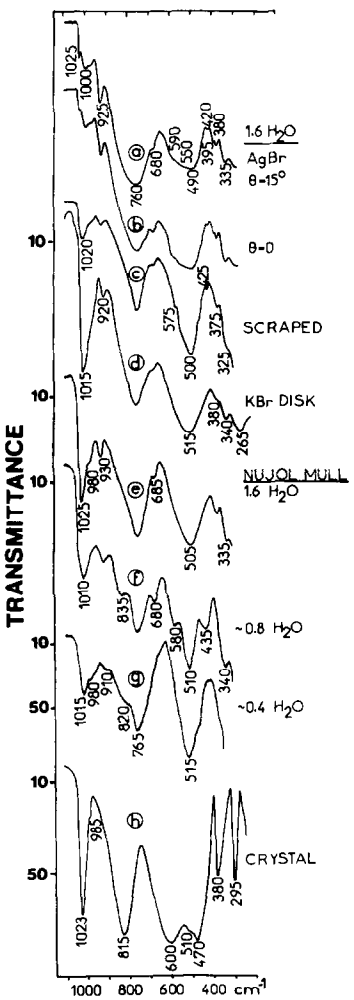

FIG. 4. Infrared spectra of xerogels under different conditions and in different media. (a) Oriented film on AgBr disk. $\theta \simeq 15°$ (see Fig. 3 for θ definition). (b) the same with θ = 0, (c) the same after scraping of the sample, (d) xerogel powder dispersed in KBr, (e) the same dispersed in Nujol, (f) the same dispersed in Nujol and heated at 100°C, (g) the same dispersed in Nujol and heated at 150°C, (h) polycrystalline V_2O_5 dispersed in KBr.

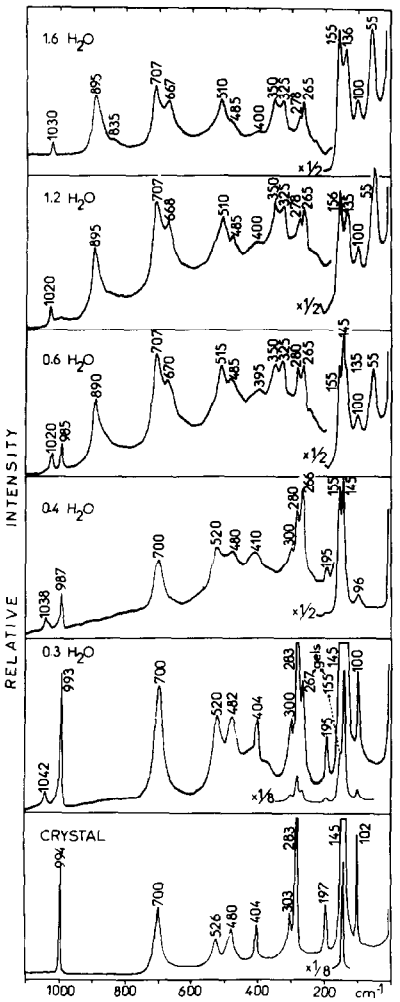

FIG. 5. Raman spectra of the xerogels (powder) $V_2O_5 \cdot nH_2O$ with n = 1.6, 1.2, 0.6, 0.4, and 0.3 compared with crystal spectrum.

which disappear or appear above a given value of n (see Table I). The Raman spectrum for $n = 0.3$ is very similar to that of the crystal, all the bands of the crystal are present, in addition we observe a weak shoulder at 155 cm^{-1} and two bands at 267 and 1042 cm^{-1}. The two first features are present up to $n = 1.6$, while the last one disappears above $n = 0.6$ and is replaced by the 1020-cm^{-1} band. In the same way for $n > 0.6$ seven new bands appear. The strongest ones observed at 55 and 890 cm^{-1} are located in new frequency ranges and this indicates that a structural modification has taken place.

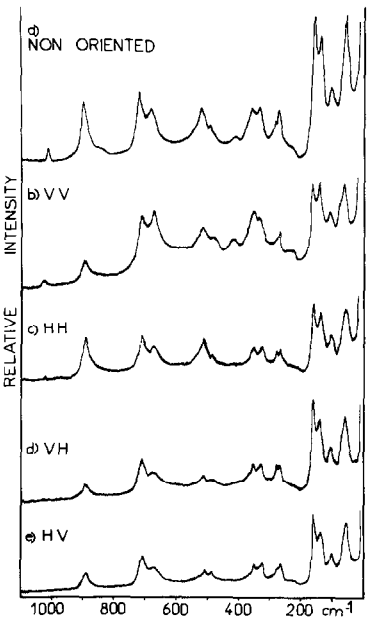

FIG. 6. Polarized Raman spectra of an oriented film of the 1.6 H_2O gel compared with a xerogel powder spectrum.

Thus the $n = 0.3$ and $n = 0.6$ composi-

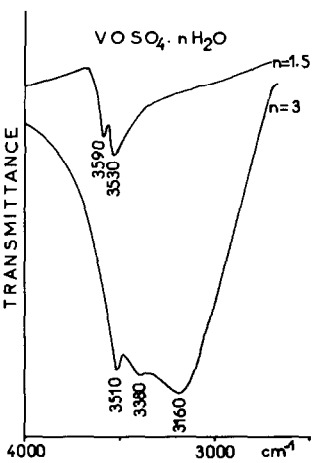

FIG. 7. Infrared spectra (4000–2500 cm^{-1}) of $VOSO_4 \cdot 3\ H_2O$ (after Tachez *et al.* (*14*)) and $VOSO_4 \cdot 1.5\ H_2O$.

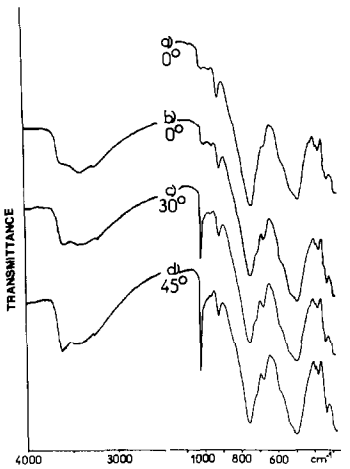

FIG. 8. (a) The sample is unidirectionally oriented in an horizontal direction and $\theta = 0°$. (b) The sample is unidirectionally oriented in a vertical direction and $\theta = 0°$. (c) Same as (b) but with $\theta = 30°$. (d) Same as (b) but with $\theta = 45°$. θ is the angle between the normal of the gel support N and the ir beam direction I: $\theta = (N, I)$.

tions appear as two blurred limits. As already stated, below 0.3 the structure is unstable and the crystal is formed, however for $0.3 < n < 0.6$ the Raman spectrum is a mixture of $n = 0.3$ and 0.6 spectra (see $n = 0.4$ in Fig. 5), the coexistence of two "phases" seems to be also observed near the exact composition $n = 0.6$, the corresponding spectrum still contains some traces of the $n = 0.3$ strongest bands (e.g., 985, 280, 145 cm^{-1}), however for $n > 1$ these bands are completely removed and are replaced by different bands which persist up to $n > 1100$ (colloidal solutions) (*15*).

(*b*) *Polarization.* X-Ray diffraction experiments and ir results [see Section 2(c) and Ref. (*12*)] have shown that evaporated gels are made of layers parallel to the support and thus it was interesting to take advantage of this to obtain polarized Raman spectra.

A gel $n = 300$ H_2O was deposited on two glass tubes; one of them was previously unidirectionally rubbed, in order to induce the alignment of V_2O_5 ribbons perpendicularly to the rotation axis of the tube. This treatment is usually done for orienting liquid crystals. These samples were then dried at 300 K so as to reach the $n = 1.6$ H_2O composition. The Raman spectra of the "oriented" and "nonoriented" ribbons present quite a similar polarization behavior. The low-frequency region below 200 cm^{-1} is not very sensitive to the polarization effect. The 50-cm^{-1} band seems to be a bit stronger in VV and HH spectra for the "oriented" ribbons than for the second sample and a small intensity decrease is observed in VH and HV spectra (see Fig. 6a). If one takes the 180-cm^{-1} band as an internal standard, the I_{VV}/I_{HH} depolarization ratios vary from 0.57 for the 895-cm^{-1} band to 2.1 for the 670- and 350-cm^{-1} bands. Moreover, the Raman spectra of a $n = 1.6$ nonoriented gel investigated in its powder form is also very similar to those of oriented layers (see Fig. 6b). This limited polarization effect is due to the fact that the out-of-plane

TABLE I

Raman frequencies					
Crystal	Xerogels				
$n = 0.0$	$n = 0.3$	0.4	0.6	1.2	1.6
			55(m)	55(s)	55(s)
102(m)	100(m)	96(w)	100(w)	100(w)	100(w)
			135(sh)	135(s)	135(s)
145(vs)	145(s)	145(s)	145(s)		
	155(sh)	155(s)	155(s)	156(s)	155(s)
197(m)	195(m)	195(w)			
	267(w)	266(m)	265(m)	265(m)	265(m)
283(s)	283(s)	280(m)	280(m)	278(w)	278(w)
303(m)	300(w)	300(sh)			
			325(m)	325(m)	325(m)
			350(m)	350(m)	350(m)
404(m)	404(m)	410(w)	395(w)	400(vw)	400(vw)
480(m)	482(m)	480(m)	485(m)	485(sh)	485(sh)
526(m)	520(m)	520(m)	515(m)	510(m)	510(m)
			670(sh)	668(m)	667(m)
700(s)	700(s)	700(m)	707(s)	707(s)	707(s)
			890(s)	895(s)	895(s)
994(s)	993(s)	987(w)	985(w)		
			1020(w)	1020(w)	1020(w)
	1042(w)	1038(w)			

Note. n: represents the number of water molecules per V_2O_5. s, strong; vs, very strong; w, weak; m, mean.

modes are certainly much weaker in Raman than the in-plane modes and that the *YY*, *ZY*, and *XY* components of the tensors associated with all the normal modes are weak. This was the case for crystalline V_2O_5 in which the $XY(B_{1g})$, $ZY(B_{3g})$, and the $YY(A_g)$ spectra were much weaker than the $ZX(B_{2g})$ and XX, $ZZ(A_g)$ spectra. On the other hand the limited range of variation for depolarization ratios indicates that either there is a stacking disorder along the *b* axis or (and) there is an orientational disorder of ribbons in the (*a*,*c*) planes. Nevertheless one can classify the bands which are enhanced in VV or HH compared to VH spectra, as due to symmetric modes. If one assumes that the ribbons keep a symmetry plane perpendicular to the layer, one can consider that these modes are of A' symmetry whereas if the crystalline symmetry is considered the diagonal spectra (VV, HH) should correspond to A_g species and VH to B_{2g} species. Thus neither precise symmetry assignments nor structural information can be drawn from the polarization data. However, one can conclude that some long-range order exists and that the ribbons are made of units with a degree of symmetry sufficient to explain the anisotropy of polarization tensors.

2. *Infrared*

(*a*) *Particle size effect.* The evolution of ir spectra of gels is not so spectacular as that of the corresponding Raman spectra, however in contrast with the Raman observations there is a strong modification of ir spectra from the crystal to the $n = 0.3$ gel (Fig. 4), e.g., thus one has to explain the shift of the absorption band at 815 down to 765 cm^{-1} (although there is no change in the Raman spectra). As already emphasized in Ref. (*7*) the particle size affects drastically the ir spectrum and in the present case it can be concluded that the dimensions of the active particles are strongly modified.

For the crystal, the strongest TO–LO splittings deduced from reflection spectra and reported at 765–959, 506–842, and 411–586 cm^{-1} (*16*) (associated with the largest oscillator strengths) correspond to the broad and strong ir absorption bands centered at about 765 and 515 cm^{-1} in the spectra of gels. Table II gives a possible interpretation of this observation. The ribbon has finite dimensions along the *a* and *b* axes of the crystal (see Fig. 2) and the vibrational excitations cannot propagate along these directions and thus some $\omega_T - \omega_L$ splittings are not expected (depending on the symmetry and their character). In such a case, corresponding ir modes are expected to be observed in a frequency range near from the "pure mechanical frequency"[1]: e.g., in the crystal when E_a is parallel to the *a* axis, the B_{3u} mode exhibits a TO–LO splitting (*16*) equal to 765–965 cm^{-1} (see Table II). For a ribbon the *L* and T_b phonons loose their character and tend toward a quasimolecular mode close to the pure mechanical frequency which, in the absence of the macroscopic electric field, is calculated at 821 cm^{-1} for the corresponding crystal mode (*7*). In agreement with what is expected, two frequencies are observed at about 821 (shoulder) and 765 cm^{-1} (strong) for the ribbon. Thus it can be concluded that the structure of the V_2O_5 gels is strongly one-dimensional and that the ribbon model proposed by Legendre *et al.* (*2*, *3*) is compatible with our results.

The half-width reductions and the appearance of shoulders and weak features in the ir spectra (Fig. 3), e.g., of gels embedded in Nujol, can also be related to variations of size of fibrils due to the departure of water. In the same way the changes between b and c spectra can also be associated with the mechanical destruction of layers of a $n = 1.6$ gel.

[1] "Pure mechanical frequency" means that the corresponding force constant is purely associated with the chemical bond.

TABLE II

CORRESPONDENCE BETWEEN INFRARED ACTIVE MODES IN V_2O_5 CRYSTAL AND THEIR COUNTERPARTS IN THE RIBBON

	V_2O_5 crystal		V_2O_5 ribbon		
	$\nu_{absorp.}$ (7)	$\nu_{reflect.}$ (16)		$\nu_{expected.}$	$\nu^{obs.}_{absorp.}$ (E//a,c)
E//c (B_{1u})		506 ω_{T_a}	ω_m	708(s)	≃680–700
		506 ω_{T_b}	ω_m	708(s)	
		842 ω_{L_c}	ω_L	844(w)	
E//a (B_{3u})	815	767 ω_{T_b}	ω_m	821(s)	765(s) 820(sh)
		767 ω_{T_c}	ω_T	767(s)	
		959 ω_{L_a}	ω_m	821(s)	
	510	411 ω_{T_B}	ω_m	534(s)	505(s) 580(sh)
		411 ω_{T_c}	ω_T	411(s)	
		586 ω_{L_a}	ω_m	534(s)	550(sh)
E//b (B_{2u})	470	473 ω_{T_a}	ω_m	476	490
		473 ω_{T_c}	ω_m	476	
		490 ω_{L_b}	ω_m	476	

Note. (i) ω_{T_a} and ω_{T_b} are the frequencies corresponding to transverse modes (E//c) propagating in the *a* and *b* directions, . . . ; (ii) ω_L: longitudinal frequency; (iii) ω_m: "pure mechanical" frequency (calculated in Ref. (11)). Because of the finite dimensions of the ribbon in the "*a*" and "*b*" directions some of the T and L modes cannot be defined and the corresponding frequencies tend toward the pure "mechanical frequency" deriving only from the chemical bond without taking into account the macroscopic electric field.

(*b*) *Host medium effect.* The ir maxima shift slightly, depending if the sample is deposited on an AgBr surface or is embedded in Nujol or in KBr. This effect is related to the dielectric constant of the respective host media (7).

(*c*) *Dichroic effects.* Figure 8 reports the effect of the orientation θ of the normal of the gel support relative to the beam direction. The strong 1025-cm^{-1} component visible for unoriented samples (dispersed in KBr or Nujol) is not observed for $\theta = 0°$, while it is strongly enhanced for $\theta = 45°$. This effect is also visible for $\theta = 15°$ (see Fig. 4a). A similar dichroic effect although much less pronounced is also observed for the 3590-cm^{-1} component.

The 1025-cm^{-1} band, in the crystal, is assigned to a B_{2u} $\nu(V{\equiv}O_A)$ stretching mode (the atomic displacements and the dipole moments are perpendicular to the layers) and it can be concluded that the dichroism associated with the corresponding band in the gel indicates that there are V≡O bonds also perpendicular to the layers stacked along the *c* axis. When the stacking order is destroyed (either by scraping the deposit on the AgBr face (see Fig. 4c), or after grinding, see Fig. 4, spectra d and e) the intensity and the half-width of the 1025-cm^{-1} band are strongly enhanced, correlatively the 505-cm^{-1} band seems to follow the same trend. The B_{2u} mode which is placed in the crystal at 470 cm^{-1} could give rise to this band in the gel (see Table II). It should correspond to an out-of-plane $\delta(VO_BV)$ bending mode and this confirms that the layers in the gel are organized in a similar way as in the crystal. On the contrary the 765-cm^{-1} band should correspond to one in-plane

mode. The intensity of this band varies when a unidirectionally oriented sample (following the same procedure as in Raman) is rotated around the normal to its surface (Fig. 8); this confirms that, the ir beam being 8% vertically polarized, there is a trend toward a uniaxial ordering in the plane of the layer, and that for this mode the dipole variation is likely parallel to the long axis of the fibril. The above remark is consistent with the correspondence between the B_{3u} crystal mode and the 765-cm^{-1} observed band reported in Table II. Finally, the 3590-cm^{-1} ir band can be assigned either to an asymetric $\nu_a(OH_2)$ stretching mode or more likely to an OH vibrator of a water molecule nonperturbed by H bonding; for such a model one expects that the ir intensity ratio for $\theta = 45$ and 0° is of about cos 45° = 0.7. The observed dichroic ratio ($D^{45}/D^0 = 0.5$) agrees with this model when one takes into account the increase of the apparent sample thickness for $\theta = 45°$.

3. *Qualitative Assignments*

As already stated in Section 2c, the stretching $\nu(V{\equiv}O_A)$ vibrations give rise to the narrow ir and Raman bands between 990 and 1050 cm^{-1}. In addition to the Raman line already observed at 995 in the crystal, a new line at 1042 cm^{-1} appears, on the spectra of the $n = 0.3$ gel, this "blue" shift indicates that some $V{\equiv}O_A$ bonds are strengthened, they could correspond to VO_5 pyramid in which one equatorial V–O bond is broken. In the $n = 0.6$ gel, these two frequencies slightly decrease to 985 and 1020 cm^{-1}, respectively, while a new intense line appears at 895 cm^{-1}. This frequency is high enough to indicate that it belongs also to a multiple $V{\equiv}O_A$ bond; its lowering, compared to 995 cm^{-1} could be associated with the fixation of water molecules on the V_2O_5 fibril skeleton; there are two possibilities: hydrogen bonding with O_A atoms, which should partly block the motions of these atoms, or more likely formation of coordination bonds with vanadium atoms which should weaken the $V{\equiv}O_A$ bonds (π back donation).

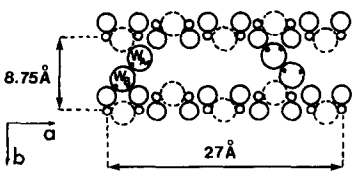

FIG. 9. Organization of water molecules in the Legendre *et al.* structural model of a $V_2O_5 \cdot 0.6\ H_2O$ "ribbon." W_A: water molecule coordinated on axial vanadium (V_A) atoms. W_B: water molecule hydrogen bonded to oxygen (O_B) atoms. Small dark circles: hydrogen atoms of W_A and W_B water molecules. Small open circles: vanadium atoms. Large open circles: O_A oxygen atoms. Large dotted circles: O_B oxygen atoms.

In that case if one refers to ir data on $[M(H_2O)_6]^{2+}$ salts (*17*) one expects $V{-}OH_2$ stretching frequencies at about 350–500 cm^{-1}. Actually new Raman bands are observed for $n > 0.6$ (Fig. 5) and the corresponding ir active modes could be overlapped by the δ(OVO) mode at 505 cm^{-1}. The existence of such an axial water molecule implies that it plays a particular role and that it could be characterized in the corresponding OH stretching region. If one tries to combine the basal spacing of 8.75 Å with the $n = 0.6$ composition, the model given in Fig. 9 seems highly probable, moreover it is shown that the occurrence of a free OH vibrator is possible. The narrow absorption band at about 3600 cm^{-1} could be characteristic of this type of coordinated water molecules noted W_A, nearly free of hydrogen bonding. Such a band is clearly observed for $n = 1.6$, it is still present for $n = 0.6$ but it does not exist for $n < 0.6$. Tachez and Theobald (*18*) have studied the structure of $VOSO_4 \cdot 1.5\ H_2O$ and they have suggested that water molecules are coordinated axially to vanadium atoms. The great similarity between the 3600-cm^{-1} ir region of this compound (Fig. 7) and of V_2O_5 gels is a further proof of the probable existence of axial H_2O molecules for $n >$

0.6. On the other hand, the broad absorption band observed below 3580 cm^{-1} is characteristic of hydrogen-bonded water molecules either with oxygen atoms of V_2O_5 or of H_2O molecules. This broad band is observed on all the spectra, and thus this type of water molecules exists in all the gels.

A certain number of Raman bands such as those at about 700, 500, and 100 cm^{-1}, are observed in the same frequency range as for the crystal and they involve likely similar internal modes, this point will be confirmed by normal mode calculations (*9*).

V. Conclusions

The vibrational spectra of the xerogels $n = 1.6$, $n = 1.2$, $n = 0.6$, $n = 0.4$, and $n = 0.3$, show in agreement with diffraction conclusions that these gels are made of layers in which the short order is closely related to those of crystalline V_2O_5. The existence of finite dimensions in the *a* and *b* directions has been correlated with the disappearance of some T–L splittings.

The spectra of the $n = 0.3$ gel are very similar to those of the crystal. Water molecules are hydrogen bonded and there are two possibilities: either they link two fibrils together as stated by Legendre *et al.* (*3*), or they are trapped into the large cavities of the V_2O_5 crystals made of 4 O_A and 4 O_B oxygens, they should be doubly bonded to the oxygen lattice by their two hydrogen atoms. DTA measurements have shown that the last 0.3 H_2O molecules leave the structure only at 510 K just before the crystallization and thus, that they are strongly retained. This can be explained by assuming either that these molecules are strongly bonded or that they are trapped during the dehydration process. The ir absorption band, characteristic of the ν(OH) vibration of these molecules, clearly shows that these molecules are weakly hydrogen bonded and therefore the second hypothesis, of H_2O molecules in cavities, seems more reasonable. If this last water had to play a interfibril bonding role it would be strongly hydrogen bonded and its ν(OH) frequency would be much more perturbed. Moreover, we have stated that the $n = 0.3$ compound has a structure very close to that of the crystal and it is reasonable to consider that the interlayers bonding are regenerated and that H_2O molecules can be trapped during the reconstruction process.

For $n = 0.6$ the V=O---V bridges must not exist, the interlayer distance being equal to 8.75 Å and thus the layers must be nearly independent. This modification of interlayer cohesion is actually responsible for the large spectral changes observed for $n = 0.6$. For this composition an additional second type of water molecules was evidenced, it should be coordinated to vanadium atoms.

Above this concentration, the maximum of the ir absorption band at about 3500 cm^{-1} is displaced toward low frequencies and this indicates that a third kind of water molecules is present. The ir data indicate that for $n > 1.6$ the hydrogen bonding is of the same order of magnitude whatever the concentration in water is.

Finally, the $n = 1.6$ compound could be described as an intermediate situation between the colloidal solution and the $n = 0.6$ compound as far as the short-range order is considered. In other words, we do not observe a marked spectral change associated with the $n = 1.4$ composition but the reduction of the 3600-cm^{-1} ir shoulder is characteristic of relatively free H_2O. This could correspond to the filling of the interlayer space available to H_2O, the excess of H_2O being involved to surround each ribbon. Finally, it must be emphasized that the water molecules for a given phase can be considered as randomly distributed over given sites and that for a given composition one can have a coexistence of two distinct

structures with the same composition, e.g., (i) for $n = 1.2$ one can describe the gel as a mixture of phase II (8.75 Å) and phase I (11.55 Å) in equilibrium, (ii) for $n = 0.4$ one can have a mixture of phase III (≃5 Å) and of phase II (8.75 Å), both of them containing 0.4 mole of H_2O per V_2O_5.

Finally the stability domain for each phase is centered around a given n but the half-width Δn of the corresponding distribution at the difference with an hydrate may be very broad.

References

1. P. ALDEBERT, N. BAFFIER, N. GHARBI, AND J. LIVAGE, *Mater. Res. Bull.* **16,** 669 (1981).
2. J. J. LEGENDRE AND J. LIVAGE, *J. Colloid Interface Sci.* **94,** 75 (1983).
3. J. J. LEGENDRE, P. ALDEBERT, N. BAFFIER, AND J. LIVAGE, *J. Colloid Interface Sci.* **94,** 84 (1983).
4. N. GHARBI, C. SANCHEZ, J. LIVAGE, J. LEMERLE, L. NEJEM, AND J. LEFEBVRE, *J. Inorg. Chem.* **21,** 2758 (1982).
5. P. ALDEBERT, H. W. HAESSLIN, N. BAFFIER, AND J. LIVAGE, *J. Colloid Interface Sci.* **98,** 478 (1984).
6. L. ABELLO AND C. POMMIER, *J. Chim. Phys.* **80**(4), 373 (1983).
7. L. ABELLO, E. HUSSON, Y. REPELIN, AND G. LUCAZEAU, *Spectrochim. Acta Part A* **39**(7), 641 (1983).
8. C. SANCHEZ, J. LIVAGE, AND G. LUCAZEAU, *J. Raman Spectrosc.* **12**(1), 68 (1982).
9. E. HUSSON, Y. REPELIN, L. ABELLO, AND G. LUCAZEAU, submitted.
10. L. ABELLO, E. HUSSON, Y. REPELIN, AND G. LUCAZEAU, "Proceedings, 8th International Conference of Raman Spectroscopy" (Bordeaux), Sept. 1982.
11. L. ABELLO, E. HUSSON, Y. REPELIN, AND G. LUCAZEAU, R. C. P. (Paris), March 1983.
12. M. T. VANDERBORRE, R. PROST, E. HUARD, AND J. LIVAGE, *Mater. Res. Bull.* **18**(9), 1133 (1983).
13. J. LEMERLE, L. NEJEM, AND J. LEFEBVRE, *J. Chem. Res.*, Miniprint, 5301 (1978).
14. M. TACHEZ, F. THEOBALD, AND R. MERCIER, unpublished results.
15. L. ABELLO AND G. LUCAZEAU, *J. Chim. Phys.* **81**(8), (1984).
16. P. CLAUWS AND J. WENNIK, *Phys. Status Solidi B* **76,** 707 (1976).
17. I. NAKAGAWA AND T. SCHIMANOUCHI, *Spectrochim. Acta* **20,** 429 (1964).
18. M. TACHEZ AND F. THEOBALD, *Acta Crystallogr. Sect. B* **36,** 2873 (1980); M. TACHEZ, thesis, no. 139, Besançon (1981).